International Journal of Computational Mathematics and Scientific Computing

DOI: 10.5281/zenodo.22310328 | ISSN: 3141-643 | Volume: 1 | Issue: 3 | 2026

Ordinary Differential Equation Models of Chemical Kinetics, HIV-Prevention Pathways, Epidemic Spread, and Growth-Decay Processes

Etim Uduak James[1]

[1]Akwa Ibom State University, Nigeria
Corresponding Author: uduakjamesetim@gmail.com

Abstract

Ordinary differential equations provide a common language for representing rates of change in chemical, biological, epidemiological, and financial systems. This study develops and computationally examines four model families drawn from physical and life-science applications: the dimensionless Lengyel-Epstein model for the chlorine dioxide-iodine-malonic acid reaction; a six-compartment demographic, exposure, infection, and AIDS-progression model motivated by delayed first sexual intercourse; the classical susceptible-infectious-removed epidemic model; and exponential growth and radioactive-decay models. Equilibria and local stability conditions are derived analytically, while numerical solutions are obtained with adaptive Runge-Kutta integration. For the chemical model with illustrative parameters a = 12 and b = 0.30, the positive equilibrium is unstable and the numerical trajectory approaches sustained oscillation. The delayed-intercourse model is locally asymptotically stable when the feedback between the sexually active and under-age compartments is weaker than total demographic removal, specifically when (d1+m1)(d2+m2+b2) > b1m1. For the epidemic illustration, the effective transmission rate is 0.8 per day, the recovery rate is 0.125 per day, and R0 = 6.4; the infectious population peaks at approximately 554 persons near day 13 in a population of 1,000. Continuous 5% financial growth increases 20,000 monetary units to 23,236.68 after three years, whereas an 800 mg bismuth-210 sample with a five-day half-life declines to 12.5 mg after 30 days. The results demonstrate how a shared differential-equation framework supports model formulation, stability analysis, simulation, and transparent comparison across distinct applications. All numerical outcomes are illustrative and are not fitted to clinical or laboratory observations.

Keywords: ordinary differential equations; mathematical modelling; chemical kinetics; HIV/AIDS; SIR model; exponential growth; radioactive decay; stability analysis

1. Introduction

Mathematical modelling converts assumptions about a real system into variables, parameters, and relations that can be analysed logically. A useful model is neither a complete replica of reality nor merely a collection of equations. It is a deliberately simplified representation designed to answer a defined question. The modelling cycle therefore involves formulation, analysis, numerical study, comparison with available evidence, and revision. Ordinary differential equations (ODEs) are especially valuable when the central question concerns how a state changes continuously with time.

ODE models have long been used in reaction kinetics, population biology, epidemiology, pharmacology, finance, and radioactive decay. Reliable numerical treatment of non-stiff initial-value problems is supported by embedded Runge-Kutta formulae with local error control [6]. The classical epidemic theory of Kermack and McKendrick [16] established a compartmental framework for transmission and removal, while later studies formalised threshold quantities such as the basic reproduction number and the next-generation operator [3, 5, 8, 15, 24]. In virology, systems of differential equations have likewise been used to relate target cells, infected cells, viruses, immune responses, and antiretroviral perturbations [9, 20-22, 25]. For nonlinear chemical systems, the chlorine dioxide-iodine-malonic acid reaction provides a canonical example in which feedback can produce oscillation and spatial pattern formation [4, 7, 17, 19, 23].

The broad value of mathematical structure is also evident in discrete and algebraic applications. Recent studies have used nilpotent groups in key-agreement protocols [13], lattices in quantum-era cryptography [11], number theory in RSA systems [12], fuzzy group actions in near-rings [14], and conjugacy classes in finitely generated groups [10]. Although those works address cryptography rather than continuous-time physical dynamics, they reinforce a common methodological point: carefully defined mathematical objects, assumptions, and transformation rules make complex systems analysable. The present study applies that principle to ODE models.

The source project considered chemical kinetics, delayed first intercourse in HIV/AIDS prevention, infectious-disease spread, and growth-decay problems separately. However, it did not provide a unified computational comparison, reproducible parameter sets, complete graphical results, or a fully correct stability argument. The present paper addresses those limitations. Its objectives are to:

1. formulate four representative ODE model families within one consistent notation;
2. derive equilibria and stability conditions where appropriate;
3. correct arithmetic and structural errors in the original calculations;
4. produce reproducible numerical simulations and graphical interpretations; and
5. distinguish clearly between theoretical illustration and empirical inference.

2. Materials and Methods

2.1. Modelling strategy

Each system was developed through six steps: identification of state variables, statement of assumptions, specification of governing equations, analytical reduction, numerical solution, and interpretation. State variables were constrained to be non-negative. Parameter values used in the simulations are illustrative values chosen to show the qualitative behaviour of the equations; they are not estimates from patients, communities, or laboratory experiments.

The nonlinear chemical and epidemic systems were solved on fixed reporting grids with an adaptive explicit Runge-Kutta method of order 5(4), using relative tolerance 10^{-9} or smaller. Embedded Runge-Kutta pairs estimate local truncation error without requiring two wholly independent integrations [6]. The linear compartment model was solved with the same method to maintain a uniform computational workflow. Population totals were not rounded during integration. Graphs were generated from the continuous numerical solutions.

2.2. Lengyel-Epstein chemical-kinetics model

The chlorine dioxide-iodine-malonic acid system can be reduced, under quasi-constant concentrations for the slower species, to two principal state variables: $X(t)$ for iodide concentration and $Y(t)$ for chlorite concentration. This family of reduced models is connected to experimental and theoretical studies of oscillation, diffusion-driven instability, and externally controlled patterning [4, 7, 17, 19, 23]. A reduced dimensional form is

$$\frac{dX}{dt} = A - BX - \frac{4CXY}{\alpha + X^2}, \qquad \frac{dY}{dt} = BX - \frac{CXY}{\alpha + X^2},$$

where A, B, C, and α are positive constants. With

$$X = x\sqrt{\alpha}, \qquad Y = \frac{\alpha B}{C} y, \qquad t = \frac{\tau}{B},$$

and dimensionless parameters

$$a = \frac{A}{B\sqrt{\alpha}}, \qquad b = \frac{C}{B\sqrt{\alpha}},$$

the kinetic equations become

$$\frac{dx}{d\tau} = a - x - \frac{4xy}{1 + x^2}, \tag{1}$$

$$\frac{dy}{d\tau} = bx\left(1 - \frac{y}{1 + x^2}\right). \tag{2}$$

For positive a and b, the interior equilibrium is

$$(x^*, y^*) = \left(\frac{a}{5}, 1 + \frac{a^2}{25}\right). \tag{3}$$

Local behaviour is determined by the eigenvalues of the Jacobian

$$J_C(x,y) = \begin{pmatrix} -1 - \dfrac{4y(1-x^2)}{(1+x^2)^2} & -\dfrac{4x}{1+x^2} \\ b\left(1 - \dfrac{y}{1+x^2}\right) + \dfrac{2bx^2y}{(1+x^2)^2} & -\dfrac{bx}{1+x^2} \end{pmatrix}. \tag{4}$$

The simulation used $a = 12$, $b = 0.30$, $x(0) = 1$, and $y(0) = 1$ over $0 \leq \tau \leq 120$.

2.3. Delayed-first-intercourse pathway model

The second system represents a demographic and disease-progression pathway rather than a complete frequency-dependent HIV transmission mechanism. Let $X(t)$ be the sexually underage population, $Y(t)$ the sexually active population, $Z(t)$ the sexually inactive population, $S(t)$ the exposed/susceptible subpopulation drawn from Y, $I(t)$ the infected population, and $A(t)$ the population with advanced AIDS. The model is

$$\begin{aligned} \frac{dX}{dt} &= b_1Y - (d_1 + m_1)X, \\ \frac{dY}{dt} &= m_1X - (d_2 + m_2 + b_2)Y, \\ \frac{dZ}{dt} &= m_2Y - d_3Z, \\ \frac{dS}{dt} &= b_2Y - (\beta + \mu)S, \\ \frac{dI}{dt} &= \beta S - (\mu + \lambda + \gamma)I, \\ \frac{dA}{dt} &= \gamma I - \lambda A. \end{aligned} \tag{5}$$

All parameters are non-negative. Here b_1 is the recruitment coefficient from Y into X through births; m_1 and m_2 are maturation/transition rates; d_1, d_2, and d_3 are demographic removal rates; b_2 is the rate of movement from Y into the susceptible/exposed state; β is the progression coefficient from S to I in this reduced chain; μ is natural mortality; γ is progression from infection to advanced AIDS; and λ is AIDS-related removal.

The coefficient matrix is block lower triangular. Four eigenvalues are immediately $-d_3$, $-(\beta + \mu)$, $-(\mu + \lambda + \gamma)$, and $-\lambda$. The remaining two are the eigenvalues of

$$M = \begin{pmatrix} -(d_1 + m_1) & b_1 \\ m_1 & -(d_2 + m_2 + b_2) \end{pmatrix}. \tag{6}$$

Consequently, the origin is locally asymptotically stable if

$$(d_1 + m_1)(d_2 + m_2 + b_2) > b_1m_1, \tag{7}$$

because the trace of M is negative and condition (7) makes its determinant positive. This corrects the source project's claim that the six eigenvalues are simply the negative diagonal entries; the coupling between X and Y cannot be ignored.

The illustrative annual parameters were $b_1 = 0.020$, $d_1 = 0.015$, $m_1 = 0.050$, $d_2 = 0.010$, $m_2 = 0.025$, $b_2 = 0.015$, $d_3 = 0.030$, $\beta = 0.080$, $\mu = 0.020$, $\gamma = 0.120$, and $\lambda = 0.100$. The initial state was $(500, 300, 100, 50, 10, 2)$ and the time horizon was 80 years.

2.4. Susceptible-infectious-removed epidemic model

For a closed population $N = S + I + R$, homogeneous mixing, constant transmission, and permanent removal after recovery, the continuous SIR system is [3, 5, 8, 15, 16, 24]

$$\frac{dS}{dt} = -\beta_e \frac{SI}{N}, \qquad \frac{dI}{dt} = \beta_e \frac{SI}{N} - \gamma I, \qquad \frac{dR}{dt} = \gamma I. \tag{8}$$

The source values specify a transmission probability of 0.08 per contact, 10 contacts per day, and an infectious duration of eight days. Thus $\beta_e = 0.08 \times 10 = 0.8$ day^{-1} and $\gamma = 1/8 = 0.125$ day^{-1}. The initial state is $(S_0, I_0, R_0) = (999, 1, 0)$ for $N = 1000$. The initial reproduction number is

$$\mathscr{R}_0 = \frac{\beta_e}{\gamma} = 6.4, \tag{9}$$

and the effective value at time t is $\mathscr{R}_e(t) = \mathscr{R}_0 S(t)/N$.

For comparison with the original discrete calculation, one forward-Euler step of length one day gives

$$S_1 = 999 - 0.8\left(\frac{999}{1000}\right) = 998.2008,$$

$$I_1 = 1 + 0.8\left(\frac{999}{1000}\right) - 0.125 = 1.6742, \qquad R_1 = 0.125. \tag{10}$$

The value 991.008 reported for the susceptible state in the source document resulted from a decimal-place error. Fractional compartment values are retained because deterministic ODE states represent expected population amounts; premature rounding distorts the dynamics.

2.5. Exponential growth and decay

If a quantity $P(t)$ changes at a rate proportional to its current value, then

$$\frac{dP}{dt} = kP, \qquad P(0) = P_0,$$

with solution

$$P(t) = P_0 e^{kt}. \tag{11}$$

For continuous financial growth, $P_0 = 20{,}000$ and $k = 0.05$ year^{-1}. For radioactive decay with half-life $T_{1/2}$,

$$\frac{dM}{dt} = -k_d M, \qquad k_d = \frac{\ln 2}{T_{1/2}}, \qquad M(t) = M_0 e^{-k_d t}. \tag{12}$$

The bismuth-210 illustration uses $M_0 = 800$ mg and $T_{1/2} = 5$ days, giving $k_d = 0.138629$ day^{-1}.

3. Results

3.1. Chemical kinetics

For $a = 12$, equation (3) gives $(x^*, y^*) = (2.4, 6.76)$. The eigenvalues of the Jacobian at this equilibrium are approximately 1.3006 and 0.4095, so the equilibrium is unstable. The trajectory moves away from the steady state and approaches a bounded oscillatory regime. Figure 1 shows repeated concentration excursions, while Figure 2 shows the corresponding closed phase trajectory. This is consistent with the capacity of the Lengyel-Epstein mechanism to exhibit oscillatory and pattern-forming behaviour [7, 17].

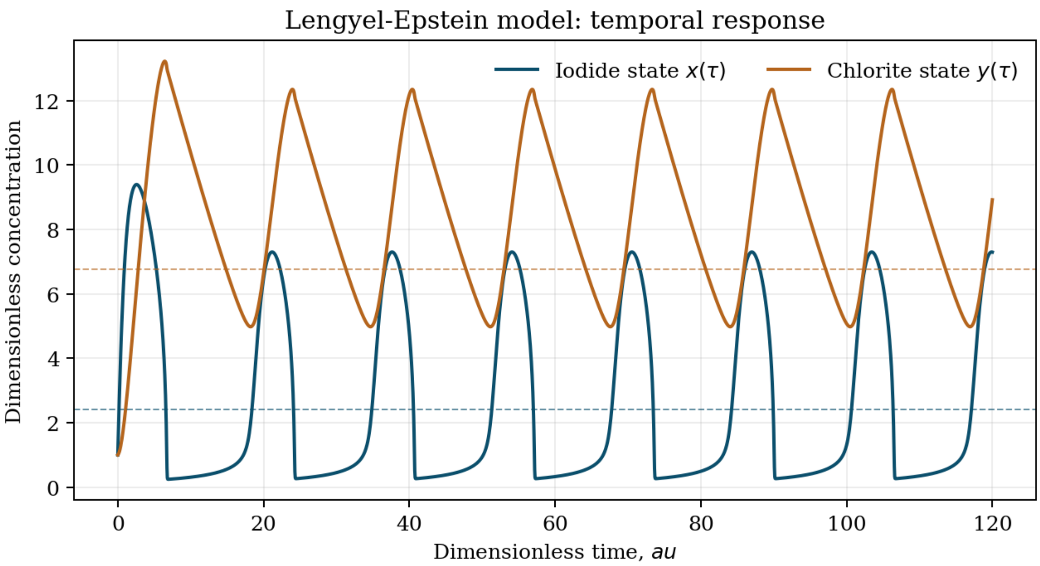

Figure 1: Temporal evolution of the dimensionless iodide and chlorite states for the Lengyel-Epstein model. Dashed lines indicate the positive equilibrium coordinates.

Figure 1. Temporal response of the dimensionless chemical-kinetics model for $a = 12$ and $b = 0.30$.

Figure 2. Phase trajectory around the unstable positive equilibrium.

3.2. Delayed-first-intercourse pathway

For the selected parameters, the X-Y block has eigenvalues -0.090 and -0.025. The remaining eigenvalues are also negative: -0.030, -0.100, -0.320, and -0.100. Therefore, all compartments decline towards the origin in the absence of external recruitment beyond the Y-to-X birth feedback represented in the system. The behaviour in Figure 3 is a consequence of the subcritical feedback condition in equation (7), not direct evidence that delaying sexual debut alone eliminates HIV.

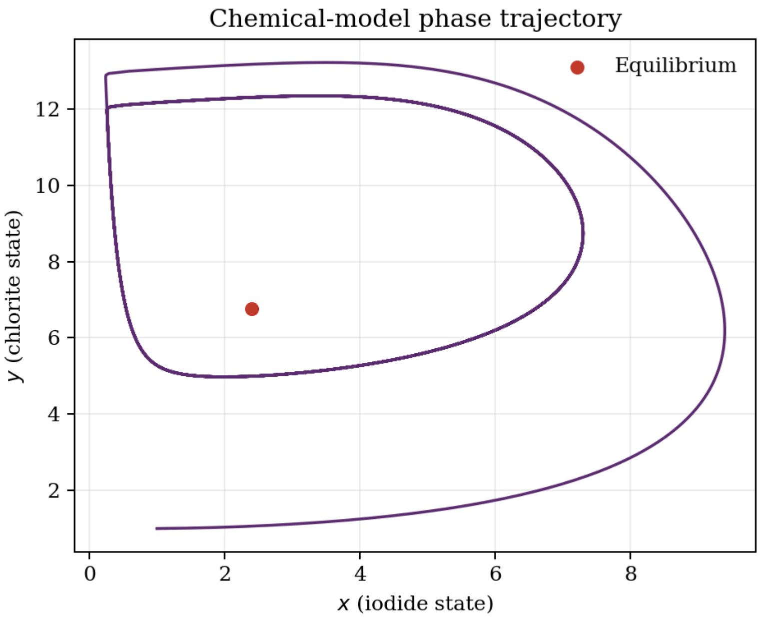

Figure 2: Phase trajectory of the chemical model in the x-y plane.

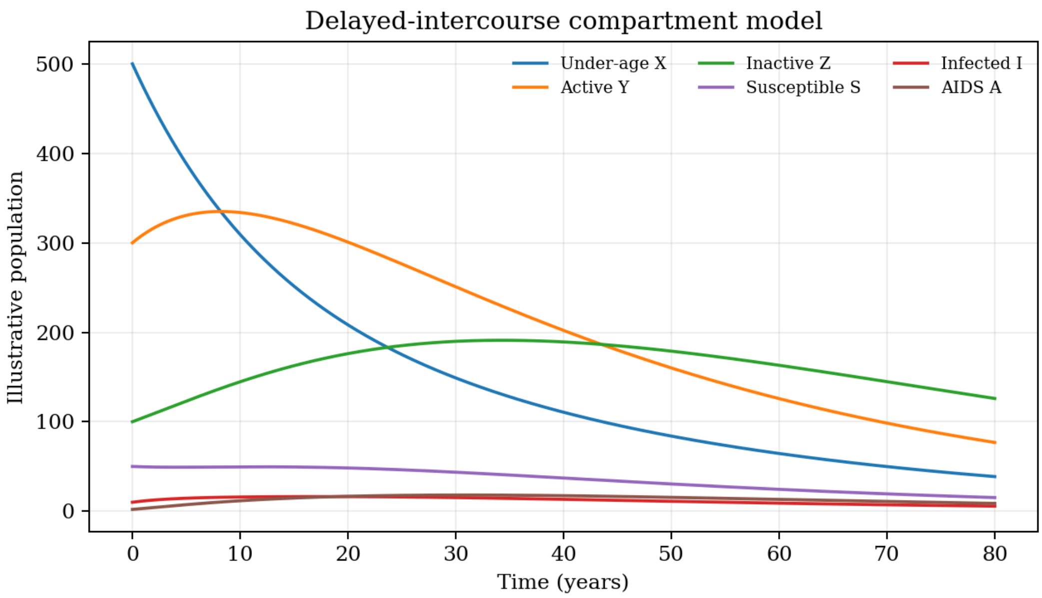

Figure 3: Numerical solution of the six-compartment delayed-intercourse pathway model.

Figure 3. Illustrative trajectories of the demographic, exposure, infection, and AIDS compartments.

3.3. Epidemic spread

Because $\mathscr{R}_0 = 6.4 > 1$, the infectious compartment initially grows. The numerical solution reaches a peak of approximately 553.9 infectious persons near day 13.0. By day 100, the solution is approximately $(S, I, R) = (1.68, 0.02, 998.31)$. The very large outbreak reflects the deliberately high effective transmission rate inherited from the source assumptions and should not be interpreted as an estimate for smallpox or any contemporary population.

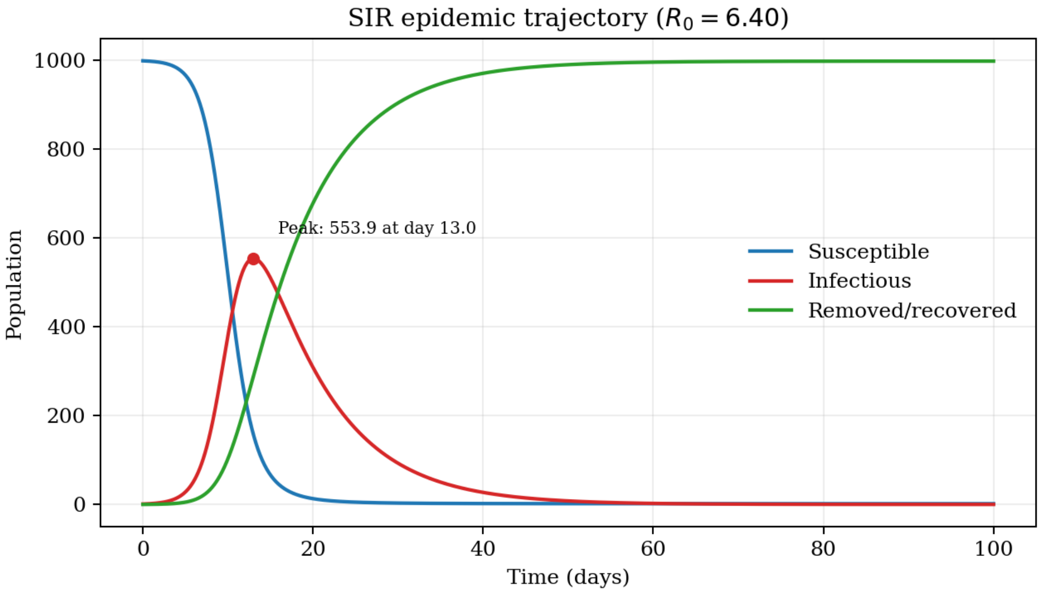

Figure 4: SIR trajectories showing susceptible, infectious, and removed populations.

Figure 4. SIR epidemic trajectory for $N = 1000$, $\beta_e = 0.8$ day^{-1}, and $\gamma = 0.125$ day^{-1}.

3.4. Growth and decay

Equation (11) yields

$$P(3) = 20{,}000e^{0.05(3)} = 23{,}236.68.$$

Thus, continuous compounding at 5% increases the balance by 3,236.68 monetary units over three years. For bismuth-210,

$$M(t) = 800e^{-0.138629t} = 800\,2^{-t/5}. \tag{13}$$

The mass is 400 mg after five days, 100 mg after 15 days, and 12.5 mg after 30 days. Figure 5 contrasts the convex growth curve with exponential decay.

Figure 5. Exponential growth and decay under the stated initial conditions.

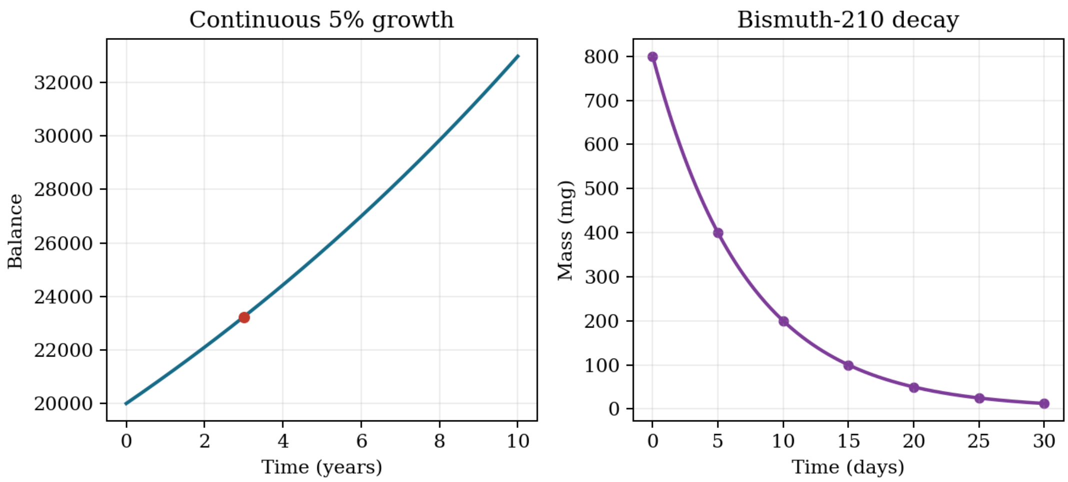

Figure 5: Continuous financial growth and bismuth-210 decay curves.

3.5. Comparative summary

Model	Governing feature	Analytical indicator	Numerical behaviour
Lengyel-Epstein kinetics	Nonlinear rational feedback	Positive equilibrium; Jacobian eigenvalues	Sustained bounded oscillation for the selected parameters
Delayed-intercourse pathway	Linear compartment chain with demographic feedback	Condition $(d_1+m_1)(d_2+m_2+b_2) > b_1 m_1$	All compartments decline under the illustrative subcritical parameters
SIR epidemic	Nonlinear mass-action incidence	$\mathscr{R}_0 = \beta_e/\gamma$	Rapid epidemic with peak near day 13 when $\mathscr{R}_0 = 6.4$
Growth-decay	Scalar linear ODE	Sign and magnitude of k	Monotone exponential increase or decrease

4. Discussion

The four applications demonstrate that similar differential-equation language can produce qualitatively different dynamics. A scalar linear equation yields a monotone exponential curve, a linear compartment system is governed by matrix eigenvalues, and nonlinear two- or three-state systems can generate oscillations and epidemic thresholds. Model behaviour therefore depends not merely on the number of variables but on feedback structure, conservation relations, parameter scales, and nonlinear coupling.

The chemical model shows why numerical analysis is essential even when an equilibrium is available in closed form. The equilibrium in equation (3) does not describe the long-run trajectory for the selected parameters because its eigenvalues are positive. The resulting oscillation is a system property generated by chemical feedback, consistent with the role of the chlorine dioxide-iodine-malonic acid reaction as a paradigm for nonlinear pattern formation [7, 17].

The HIV-prevention formulation requires more caution. As written, equation (5) does not contain a conventional force of infection such as $\beta SI/N$ or a contact function that depends on the infected population. Its parameter β is therefore a transition coefficient in a one-way exposure/progression chain, not a complete transmission parameter. The model can illustrate how delayed entry into a sexually active class reduces downstream flow, but it cannot estimate intervention effectiveness without age-specific demographic data, sexual-contact structure, infection prevalence, and calibration. Mechanistic within-host HIV models use viral-load and target-cell data to estimate turnover and treatment response [9, 20-22, 25], whereas population-level transmission models use contact and infection processes; the two scales answer different questions and should not be conflated.

The corrected SIR calculation illustrates the sensitivity of recursive models to arithmetic accuracy. A misplaced decimal changed the first susceptible update by more than seven persons. In addition, rounding $I_1 = 1.6742$ to one person before the next step would introduce avoidable numerical error. Compartment values in deterministic models are expectations or population densities; they need not be integers at intermediate times. The continuous simulation also recovers the classical threshold principle: infection grows initially when $\mathscr{R}_0 S_0/N > 1$ [3, 5, 8, 15, 16, 24].

The five algebraic and cryptographic studies included in this paper [10-14] concern different application domains, but they share the need for precise definitions and internally consistent operations. Nilpotent groups, lattices, modular arithmetic, near-rings, and conjugacy classes are not inputs to the present ODE simulations. They are cited as related examples of mathematical structure supporting applied problem solving, thereby avoiding a false claim that they validate the biological or chemical models.

5. Limitations

This study is theoretical and computational. No laboratory concentration series, epidemiological surveillance data, behavioural survey, or financial transaction data were fitted. Consequently, the simulations demonstrate model behaviour but do not provide forecasts. The chemical reduction assumes that several reactant concentrations remain effectively constant. The delayed-intercourse system omits partnership networks, sex and age heterogeneity, treatment, vertical transmission, migration, and a prevalence-dependent force of infection. The SIR model assumes homogeneous mixing, a closed population, and permanent removal. Parameter uncertainty and sensitivity were not estimated. Finally, the continuous compounding example is pedagogical and excludes fees, taxes, inflation, and changing interest rates.

6. Conclusion

This paper transformed four classroom-style formulations into a unified, reproducible ODE study. The analysis produced an unstable equilibrium and oscillatory solution for the selected Lengyel-Epstein parameters, established the correct stability condition for the coupled demographic block of the delayed-intercourse pathway, corrected the first-step SIR arithmetic, and derived the standard growth and decay solutions. The computational graphs make the consequences of each model's assumptions visible. The principal methodological conclusion is that model equations must be interpreted together with their assumptions, parameter meanings, stability properties, and data limitations. Future work should calibrate each model separately with domain-specific observations and quantify parameter uncertainty before prediction or policy use.

Funding

The author received no specific funding for this study.

Conflict of Interest

The author declares no conflict of interest.

Data and Code Availability

The results are generated from the equations and parameter values reported in the paper. The accompanying script reproduces all numerical solutions and figures.

Ethics Statement

No human participants, patient records, animals, or personally identifiable data were used.

References

[1] Allen, L. J. S. (1994). Some discrete-time SI, SIR, and SIS epidemic models. *Mathematical Biosciences, 124*(1), 83-105. https://doi.org/10.1016/0025-5564(94)90025-6

[2] Allen, L. J. S., & Burgin, A. M. (2000). Comparison of deterministic and stochastic SIS and SIR models in discrete time. *Mathematical Biosciences, 163*(1), 1-33. https://doi.org/10.1016/S0025-5564(99)00047-4

[3] Anderson, R. M., & May, R. M. (1991). *Infectious diseases of humans: Dynamics and control*. Oxford University Press.

[4] De Kepper, P., Castets, V., Dulos, E., & Boissonade, J. (1991). Turing-type chemical patterns in the chlorite-iodide-malonic acid reaction. *Physica D: Nonlinear Phenomena, 49*(1-2), 161-169. https://doi.org/10.1016/0167-2789(91)90204-M

[5] Diekmann, O., Heesterbeek, J. A. P., & Metz, J. A. J. (1990). On the definition and the computation of the basic reproduction ratio R_0 in models for infectious diseases in heterogeneous populations. *Journal of Mathematical Biology, 28*(4), 365-382. https://doi.org/10.1007/BF00178324

[6] Dormand, J. R., & Prince, P. J. (1980). A family of embedded Runge-Kutta formulae. *Journal of Computational and Applied Mathematics, 6*(1), 19-26. https://doi.org/10.1016/0771-050X(80)90013-3

[7] Ghosh, P., Sen, S., Riaz, S. S., & Ray, D. S. (2009). Galerkin analysis of light-induced patterns in the chlorine dioxide-iodine-malonic acid reaction-diffusion system. *Physical Review E, 79*(5), 056216. https://doi.org/10.1103/PhysRevE.79.056216

[8] Hethcote, H. W. (2000). The mathematics of infectious diseases. *SIAM Review, 42*(4), 599-653. https://doi.org/10.1137/S0036144500371907

[9] Ho, D. D., Neumann, A. U., Perelson, A. S., Chen, W., Leonard, J. M., & Markowitz, M. (1995). Rapid turnover of plasma virions and CD4 lymphocytes in HIV-1 infection. *Nature, 373*, 123-126. https://doi.org/10.1038/373123a0

[10] John, M. N., Musa, A., & Udoaka, O. G. (2023a). Conjugacy classes in finitely generated groups with small cancellation properties. *European Journal of Statistics and Probability, 12*(1), 1-9. https://doi.org/10.37745/ejsp.2013/vol12n119

[11] John, M. N., Ogoegbulem, O., Obi, P. N., Egbogho, H. E., & Udoaka, O. G. (2023b). Lattices in quantum-era cryptography. *International Journal of Research Publication and Reviews, 4*(11), 2175-2179. https://doi.org/10.5281/zenodo.10207209

[12] John, M. N., Ogoegbulem, O., Obukohwo, V., & Egbogho, H. E. (2023c). Number theory in RSA encryption systems. *GPH-International Journal of Mathematics, 6*(11), 7-16. https://doi.org/10.5281/zenodo.10209900

[13] John, M. N., Udoaka, O. G., & Musa, A. (2023d). Nilpotent groups in cryptographic key exchange protocol for $N \geq 1$. *Journal of Mathematical Problems, Equations and Statistics, 4*(2), 32-34. https://doi.org/10.22271/math.2023.v4.i2a.103

[14] John, M. N., & Udoakpan, I. U. (2023e). Fuzzy group action on an R-subgroup in a near-ring. *International Journal of Mathematics and Statistics Studies, 11*(4), 27-31. https://doi.org/10.37745/ijmss.13/vol11n42731

[15] Keeling, M. J., & Rohani, P. (2008). *Modeling infectious diseases in humans and animals*. Princeton University Press. https://doi.org/10.1515/9781400841035

[16] Kermack, W. O., & McKendrick, A. G. (1927). A contribution to the mathematical theory of epidemics. *Proceedings of the Royal Society A: Mathematical, Physical and Engineering Sciences, 115*(772), 700-721. https://doi.org/10.1098/rspa.1927.0118

[17] Lengyel, I., & Epstein, I. R. (1991). Modeling of Turing structures in the chlorite-iodide-malonic acid-starch reaction system. *Science, 251*(4994), 650-652. https://doi.org/10.1126/science.251.4994.650

[18] Murray, J. D. (2002). *Mathematical biology I: An introduction* (3rd ed.). Springer. https://doi.org/10.1007/b98868

[19] Muñuzuri, A. P., Dolnik, M., Zhabotinsky, A. M., & Epstein, I. R. (1999). Control of the chlorine dioxide-iodine-malonic acid oscillating reaction by illumination. *Journal of the American Chemical Society, 121*(35), 8065-8069. https://doi.org/10.1021/ja9910457

[20] Nowak, M. A., & May, R. M. (2000). *Virus dynamics: Mathematical principles of immunology and virology*. Oxford University Press. https://doi.org/10.1093/oso/9780198504184.001.0001

[21] Perelson, A. S. (2002). Modelling viral and immune system dynamics. *Nature Reviews Immunology, 2*(1), 28-36. https://doi.org/10.1038/nri700

[22] Perelson, A. S., Neumann, A. U., Markowitz, M., Leonard, J. M., & Ho, D. D. (1996). HIV-1 dynamics in vivo: Virion clearance rate, infected cell life-span, and viral generation time. *Science, 271*(5255), 1582-1586. https://doi.org/10.1126/science.271.5255.1582

[23] Turing, A. M. (1952). The chemical basis of morphogenesis. *Philosophical Transactions of the Royal Society of London. Series B, Biological Sciences, 237*(641), 37-72. https://doi.org/10.1098/rstb.1952.0012

[24] van den Driessche, P., & Watmough, J. (2002). Reproduction numbers and sub-threshold endemic equilibria for compartmental models of disease transmission. *Mathematical Biosciences, 180*(1-2), 29-48. https://doi.org/10.1016/S0025-5564(02)00108-6

[25] Wei, X., Ghosh, S. K., Taylor, M. E., Johnson, V. A., Emini, E. A., Deutsch, P., Lifson, J. D., Bonhoeffer, S., Nowak, M. A., Hahn, B. H., Saag, M. S., & Shaw, G. M. (1995). Viral dynamics in human immunodeficiency virus type 1 infection. *Nature, 373*, 117-122. https://doi.org/10.1038/373117a0

Journal Website: https://ktrendjournals.org/